Materials International
Open-Access Journal (ISSN: 2668-5728)

Article
Volume 7, Issue 4, 2025, 35
https://doi.org/10.33263/Materials74.035

Green Synthesis of Silver Nanoparticles from *Acacia karroo* Hayne and Their Analgesic and Anti-Inflammatory Effects.

Opeyemi Avoseh [1*], Folajimi Avoseh [2], Zechariah Oresanya [1,*], Olawale Osifeko [1], Adeniyi Adejare [1], Fanyana Mtunzi [3]

[1] Department of Chemistry, Faculty of Science, Lagos State University, Lagos, Nigeria
[2] Institute of Chemical and Biotechnology, Vaal University of Technology, Vanderbijlpark 1900, Gauteng, South Africa
* Correspondence: seavoseh@gmail.com (O.A.); zechariaholuwadamilola@gmail.com (Z.O.);

Received: 3.04.2025; Accepted: 20.07.2025; Published: 10.12.2025

Abstract: In the present study, we evaluate *Acacia karroo* (AK) leaf hydrosols' efficacy as reducing and capping agents in the synthesis of silver nanoparticles (AgNPs). The evolution of the optical and morphological properties was monitored at different temperatures and reaction times. The hydrosol and as-synthesized AgNPs were characterized by UV-visible spectroscopy (UV), attenuated total reflectance Fourier Transform- Infra-Red spectroscopy (ATR-FTIR), Scanning Electron Microscope (SEM), energy-dispersive x-ray spectroscopy (EDS), transmission electron microscope (TEM), and X-ray diffraction (XRD). The pain-mediating capacity of the AK-AgNPs was examined using the formalin-induced in vivo pain model in Swiss mice. We showed that Acacia karroo stem bark hydrosols successfully reduced and stabilized the AgNPs, with particle size and stability highly dependent on the reaction temperature and time (e.g., at 60°C, particle sizes are small and uniform (~ 17.2 ± 0.6 nm), while larger sizes are obtained at 80°C (20.1 ± 0.2 nm). Also, the AKDS-AgNPs synthesized exhibited a very high analgesic property, $p < 0.01$ at a 58% inhibition rate when used in the treatment of Swiss mice using formalin as a phlogistic agent. These findings further establish the Acacia species' potential as a precursor for silver nanoparticles' biosynthesis and their use as a potential analgesic drug.

Keywords: *Acacia karroo* Hayne; silver nanoparticles; analgesic; Swiss mice; neurogenic phase; formalin test; inflammatory.

1. Introduction

Metal nanoparticles are unique in their characteristics (optical, electronic, and catalytic) due to their small size and high surface-to-volume ratio. This uniqueness makes them susceptible to applications such as biosensors, catalysts, data storage, optics, drug delivery, packaging, and water purification. Other medical applications include fluorescent bio-labels, drug loadings, cancer therapy, and protein detection. Silver nanoparticles (Ag-NPs) have generated tremendous interest due to their vast antimicrobial, fascinating catalytic, optical, and electrical applications [1–5]. Mohamed, J., Saadh investigated the activity of Ag-NPs on the Goatpox virus (GTPV); Ag-NPs caused significant inhibition of GTPV replication by preventing virus entry into the host cell [6].

Chemical methods, commonly used to synthesize nanomaterials, pose challenges such as environmental contamination, energy consumption, and health risks. The toxic chemicals used in these methods can induce cancer, cytotoxicity, and environmental contamination, especially when organic solvents and reducing agents are involved [7,8]. Green synthetic methods that incorporate natural products, such as plants, marine, and terrestrial organisms, provide a safe and clean alternative. The bio-reductive and stabilizing potential of these natural materials is attributed to the individualistic and synergistic activities of proteins, flavonoids, terpenoids, vitamins, and tannins present in living organisms. Singh *et al*. reported the bio-reduction and capping of silver nanoparticles by clove plant (*Syzygium aromaticum*). The reaction mechanism was attributed to the inductive effects of the methoxy and allyl groups present on the eugenol molecule (the main component of the clove plant) [9]. Keto- and enol-groups of the quercetin facilitate the synthesis of Ag nanoparticles by *Ocimum basilicum* [10], employing the carbonyl and hydroxyl on C-3 and C-5, respectively, as metal chelation [11].

Silver nanoparticles synthesized from living organisms, such as plants, exhibit biological and pharmaceutical properties. Silver nanoparticles of 10-20 nm were synthesized from the root extract of Zingiber officinale and employed in the synthesis of Ag-NPs, which inhibit Staphylococcus spp. and Listeria spp. bacteria [12]. AgNPs of 5.7 ± 0.2 nm in size were synthesized from *Anogeissus latifolia*. They significantly inhibited gram-positive and gram-negative bacteria, demonstrating high antibacterial activity [13].

Inflammation is a complex biological response to harmful stimuli such as pathogens, damaged cells, or irritants, involving the release of mediators that regulate cellular infiltration and tissue repair [14]. When unresolved, chronic inflammation can contribute to various diseases [15, 16]. Conventional anti-inflammatory agents like NSAIDs and corticosteroids have long been used but are associated with significant adverse effects. NSAIDs, for instance, are linked to gastrointestinal toxicity, cardiovascular complications, renal and hepatic impairments, and hypertension [17], while corticosteroids may cause systemic immunosuppression, increased infection risk, and cartilage degeneration [18]. Historically, silver has been employed for treating inflammation and wound healing. More recently, silver nanoparticles (AgNPs) have shown promise for similar applications, both topically and intravenously [19,20]. Although their precise mechanism remains under investigation, their efficacy is thought to stem from their nanoscale size [21,22] and potential to modulate pro-inflammatory cytokines [23].

Acacia karroo Hayne, also known as sweet thorn, is a member of the Fabaceae family and is widely distributed across all nine provinces of South Africa [24]. Locally, it is prepared as a concoction to treat malaria and stomach ailments, as boiled water to treat diarrhea in goats, and as feed forage for herbivores [25]. It contains epicatechin, epigallocatechin, β-sitosterol, and high molecular mass decalin derivatives. AgNPs synthesized from *Acacia mearnsii* were highly crystalline with face-centered cubic structures with average sizes between 6-50 nm. In this study, hydrosols prepared from the stem bark of *A. karroo* were used for the biosynthesis of AgNPs. The plasmon response was monitored using UV-visible spectroscopy and morphologically characterized with SEM, EDS, TEM, and XRD. The functional group modifications were analyzed with FTIR spectroscopy. A. karroo dry stem hydrosols (AKDS) and AKDS-AgNPs were evaluated for their anti-inflammatory and antinociceptive properties in vivo using the formalin assay. In contrast to other *Acacia* species, the application of *Acacia karroo* as a bio-reductant and capping agent in the synthesis of silver nanoparticles remains underexplored. This study presents one of the first in vivo evaluations of its nanoparticle-

mediated anti-inflammatory and antinociceptive activities, highlighting its distinct phytochemical contributions.

2. Materials and Methods

2.1. Plant materials.

Acacia karroo stem bark (AKDS) (Figure 1a) were collected at Walter Sisulu University, Mthatha, Eastern Cape, South Africa (31°36'08.35" S 28°45'02.48" E) botanical garden and was taxonomically identified at Selmar Schonland Herbarium, Grahamstown (GRA), South Africa by Mr. T. Dold; voucher sample was deposited, and voucher number (AOK001) was collected at the herbarium.

2.2. Chemicals and reagents.

Silver nitrate ($AgNO_3$) was obtained from Sigma-Aldrich and used as acquired. The hydrosol prepared from *Acacia karroo* leaves aided in the reduction and passivation of the $AgNO_3$.

2.3. Preparation of the hydrosol of Acacia karroo.

The hydrosol was prepared by subjecting about 300 g of dried stem bark to hydro-distillation using a Clevenger-type apparatus. Upon completion of essential oil extraction, the flask extract was allowed to cool, filtered, and kept for analysis. The extract was used after three days of preparation to prevent photooxidation and mucus growth on the extract.

2.4. Synthesis of (AKDS)-AgNPs.

Approximately 50 mL of the AKDS hydrosol was transferred into a three-necked flask fitted with a temperature sensor and positioned in a jacketed heating mantle with a magnetic stirrer. An aqueous solution of $AgNO_3$ at 0.1 mol/L, 10 mL, was added to the flask, stirred, and heated to 60°C and 80°C. To avoid the auto-reduction of AgNO3 by photosensitivity, the flask was covered with aluminum foil and placed in a dark cupboard until the reaction was complete. Color change from dark brown to greyish color (Figure 1) provides evidence of reduction.

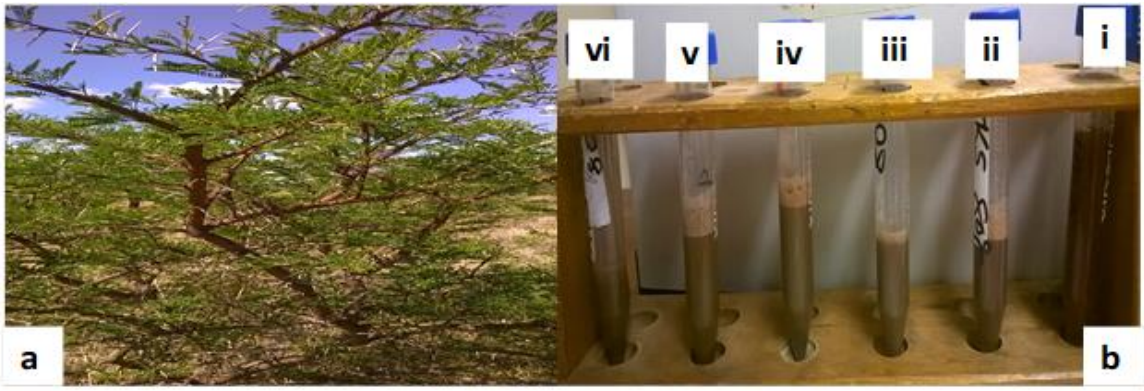

Figure 1. (a) *Acacia karroo* plant; **(b)** Color change of extract **(i)** before synthesis; **(ii)** 15 mins; **(iii)** 30 mins; **(iv)** 3 h; **(v)** 4 h; **(vi)** 21 h.

The bio-reduction and stability of Ag-NPs in the colloidal solution were examined at 15 min, 30 min, 60 min, and 3h by sampling of 2.0 mL aliquots of the solution on a UV−visible

(UV−vis) spectrophotometer (SHIMADZU model UV-1650 PC, Japan) in the range of 200-900 nm.

2.5. Phytochemical screening of AKDS hydrosol.

To determine the presence of terpenoids, alkaloids, tannins, flavonoids, phenols, reducing sugars, and saponins, an aliquot of the hydrosol was analyzed according to Mogole (2020) [26].

2.5.1. Alkaloids.

Alkaloids were detected using Mayer's reagent method. About 0.2g of each extract was dissolved in dilute HCl and filtered. The filtrate was treated with Mayer's reagent. A yellow precipitate confirms the presence of alkaloids.

2.5.2. Reducing sugars.

Reducing sugars were detected using Fehling's reagent method. To 1mL of each extract, 5mL of distilled water was added, and the solution was filtered. Then, dilute HCl was added to the filtrate (Hydrolysis), neutralized using an alkaline solution, and then treated with Fehling's solution A and B (2 mL) in the presence of heat. The presence of a red precipitate indicates the presence of reducing sugar.

2.5.3. Saponins.

Saponins were detected using a Foam confirmatory test. Each extract weighing 0.1 g was shaken with 2 mL of distilled water. The formation of foam confirms the presence of Saponins.

2.5.4. Phenols.

Phenols were detected using the ferric chloride test. About 1 mL of each extract was treated with a few drops of $FeCl_3$ solution. The formation of a bluish-black colour confirms the presence of phenols.

2.5.5. Flavonoids.

Each extract's 1 mL was treated with 2-3 drops of 0.1M NaOH solution to produce a yellow solution. Dilute HCl was added to the solution to decolourize it. The disappearance of a yellow colour confirms the presence of flavonoids.

2.5.6. Steroids and terpenoids.

Steroids and terpenoids were detected using the Liebermann-Burckhardt test. About 1 mL of chloroform was added to 1 mL of each extract, followed by acetic acid (2-3 mL) and 1-2 drops of (conc) H_2SO_4. A dark green color confirms the presence of steroids. A pink colour confirms the presence of terpenoids.

2.5.7. Tannins.

1 mL of each extract was treated with 2-3 drops of 5% $FeCl_3$ solution. The formation of a blue-black or greenish-black coloration indicated the presence of tannins. Additionally,

1 mL of each extract was mixed with an equal volume of 1% gelatin solution containing 10% NaCl. The appearance of a white or buff-colored precipitate confirmed the presence of tannins.

2.6. Characterization.

2.6.1. UV-visible spectroscopy.

The UV–visible spectra were recorded using a UV 1650 PC-Shimadzu B UV–visible spectrophotometer (Shimadzu, Osaka, Japan).

2.6.2. Fourier transform infrared spectrophotometer analysis.

FTIR was used to analyze the biomolecules responsible for the reduction and capping of the as-synthesized AKDS-AgNPs. The FTIR spectra were obtained within the range of 370–4000 cm-−1 utilizing an FTIR spectrometer that has a universal ATR sampling accessory.

2.6.3. Scanning electron microscopy (SEM) and energy-dispersive X-ray spectrometer (EDS) analysis.

Ag-NPs were obtained from the synthesized suspension by centrifuging 5 mL of solution at 40,000 rpm (Eppendorf Centrifuge 5702 R). The fine particles obtained were dehydrated in an oven at 50°C to obtain a powdered form and were used further for EDX investigation. A powdered sample of the AKDS and AKDS-AgNPS was spread evenly on a Cu block. A JEOL JSM 6390 LV SEM at 15Kv (Japanese Electron Optical Lab.) was used for SEM analysis. The specimens were coated with a thin layer of gold to avoid charging effects.

2.6.4. XRD measurement.

The crystallinity of the AKDS-AgNPs was examined on a Bruker D8 Advanced X-ray diffractometer. The patterns were recorded at a scan speed of 4°/min with Cu Kα radiation (λ = 1.5406 Å) operated at 40 kV and 30 mA.

2.6.5. TEM analysis.

The size, shape, and morphology of as-synthesized AgNPs were observed using the Transmission electron microscope (TEM). TEM analysis was performed using a JEOL JEM 2100 (TEM) operating at 200 kV. The samples were placed on a carbon-coated copper grid and subsequently dried on filter paper.2.7. Analysis of the analgesic.

2.7.1. Ethical clearance.

An ethical clearance certificate was secured from the Research Ethical Clearance Committee (RECC) of the University (Approval no: 013/2019/LASU/BCH).2.7.2. Toxicity assay.

The physiological biosafety of AKDS and AKDS-AgNPs on Swiss mice was analyzed using 50, 100, and 200 mg/kg of the extract. A total of 25 Swiss mice, weighing 150-200 grams and representing both genders, were used in the toxicity study, organized into groups of 5 animals each. Swiss mice were administered 50, 100, and 200 mg/kg of AKDS and AKDS-AgNPs by oral route. The negative control group received normal saline.

2.7.3. Formalin assay.

The formalin test was carried out using the Prabhu *et al* method with some modifications [27]. Four groups of mice were selected for the present study and grouped as follows:

Group I:	Vehicle treated Control Group	0.09%
Group II:	Aspirin Group (standard)	10 mg/kg
Group III:	AKDS extract	200 mg/kg
Group IV:	AKDS-AgNPs	200 mg/kg

Briefly, formalin solution (1% in distilled water; 0.5 mL per paw was administered via an intraplantar injection into the hind paw of the grouped animals. The duration (in seconds) spent intensely licking or biting the injured paw was recorded during two intervals: 0–5 minutes (the first phase indicating neurogenic pain) and 15–30 minutes (the second phase indicating inflammatory pain). Oral administration of Aspirin (10 mg/kg; serving as the positive control) was also provided, along with the vehicle. (water, 10 mL/kg), AKDS (200 mg/kg) and AKDS-AgNPs (200 mg/kg) were given 60 min prior to formalin administration. The evaluation of percentage inhibitions is conducted using:

$$\text{Percentage inhibition} = [(1 - T/C)] \times 100 \quad (1)$$

From the equation, T represents the frequency at which treated Swiss mice licked or bit their injected paw, while C denotes the frequency at which control mice licked or bit the treated paw.2.7.4. Statistical analysis.

Unless stated otherwise, the data are expressed as Mean ± SEM for the assessed parameter and were subjected to statistical analysis using one-way analysis of variance (ANOVA) followed by Dunnett's multiple-comparison test for the formalin-induced assay, using GraphPad Prism (version 7.02), San Diego, CA, USA (www.graphPad.com). The lowest threshold for significance that was considered was $P < 0.05$. $P < 0.01$. was considered statistically significant between the means.

3. Results and Discussion

3.1. Phytochemical screening.

Plant materials are composed of natural products that impart pharmacological properties when either consumed by animals or humans. These phytochemicals are present in plants' specialized cells and can be released using extraction methods that involve organic solvents, high temperatures, extended sonication, and maceration. Table 1 shows the presence of alkaloids, steroids, terpenoids, flavonoids, saponins, reducing sugars, and tannins in the hydrosol of *Acacia karroo.* The hydrosol is composed mainly of high-phenolic compounds, such as flavonoids and phenols. Compounds such as epicatechin, epigallocatechin, and β-sitosterol were isolated from parts of the plant [28].

Table 1. Phytochemicals present in AKDS hydrosol.

Phytochemicals	Present or Absent (+/-)
Alkaloids	+
Steroids and Terpenoids	+
Flavonoids	+
Saponins	+
Reducing sugars	+
Tannins	+

Phytochemicals	Present or Absent (+/-)
Phenols	+

3.2. Optical characterization.

3.2.1. Ultra-violet spectroscopy.

Specific noble-metallic nanoparticles, especially Ag and Au, exhibit strong interactions with visible light, enabling electron conduction at the metal surface and leading to collective oscillation. This phenomenon, called Surface Plasmon Resonance (SPR), results in strong scattering and absorption. Specifically, AgNPs can display an effective extinction (scattering + absorption) cross-section ten times larger than their physical cross-section. This collective oscillation leads to the observed UV spectrum of a typical AgNP. Furthermore, the metal nanoparticle's resonance frequency depends on its shape, size, and type, as well as the surrounding medium.

In this study, by keeping the volume and concentration of the $AgNO_3$ precursor solution constant (10 ml, 0.1 M), the effect of temperature on the bio-reduction and stability of nanoparticles was investigated. As the reaction time increased, the solution's color shifted from dark brown to a grey-brownish color, indicating the formation of Ag-NPs (Figure 1b (image i-vi). Figure 2a and b show the UV spectra of the AKDS-AgNPs synthesized at 60°C and 80°C, respectively. In this oxidation-reduction reaction, silver nitrate serves as the oxidant, and the AKDS extract serves as the reducing and capping agent. At the same time, AKDS-AgNPs are the reducing product. A peak in surface plasmon resonance (SPR) associated with the excitation of longitudinal plasmon vibrations of silver nanoparticles (Ag-NPs) was detected at 470 nm, as shown in the SPR spectra in Figure 2A. The position of the SPR peak remains the same for the 15, 30, and 60 minutes. The steady SPR peak position and shape at these reaction times indicate a uniform size distribution. However, at the 3rd h, the SPR peak position gradually red-shifted to 474 nm, indicating an increase in particle size distribution.

On the other hand, at 80°C, the SPR peak position and shape, centered at 484 nm, remained steady across all reaction times. This could result from the stability of the AKDS-AgNPs over the reaction time. The broadening observed beyond this wavelength can be attributed to the formation of particles of different sizes, as shown in Figure 2B. AKDS-AgNPs synthesized in this reaction condition show that an increase in temperature favors the stability of the synthesized Ag-NPs. Murugan *et al*. reported size variation in *Acacia leucophlae*-AgNPs synthesized at different temperatures [29].

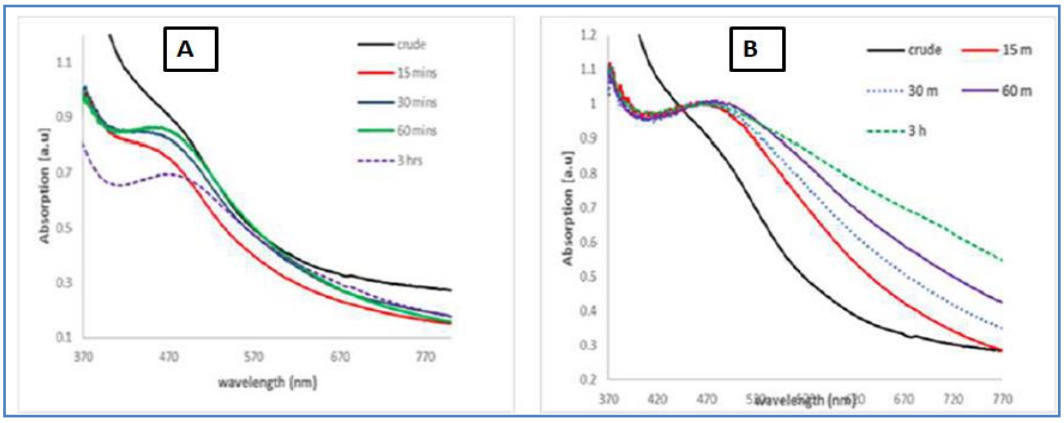

Figure 2. (A) Absorption spectra of AKDS-AgNPs synthesized using 0.1 mol/L $AgNO_3$ at 60°C; **(B)** at 80°C at different reaction times.

The SPR peak of several Acacia species has been reported; *Acacia mearnsii*-Ag-NPs were observed at 480 nm, *Acacia cyanophylla*-AgNPs at 460 nm, and *A. catechu*-AgNPs at 470 nm [30, 31]. We previously reported the stability in shape and position of the SPR peak of Acacia mearnsii silver nanoparticles synthesized at room temperature and at 40°C [32]. Increased molecular kinetic motion and a higher collision rate are the results of elevated temperature, leading to higher nucleation, whereas nanoparticles synthesized at low temperatures result in larger particle sizes [33].

3.2.2. Infra-red spectroscopy.

FT-IR spectra of the crude and as-synthesized Ag nanoparticles are shown in Figure 3, with further elucidation in Table 2. Changes in peak intensity, band shifts, and the appearance and disappearance of peaks are characteristic features of nanoparticle reduction and stabilization. The crude sample exhibits a broad absorption peak at 3409.8, characteristic of the stretching vibrations of the alcoholic groups present in flavonoids, phenols, and terpenoids of *A. karroo*. Other prominent peaks include those of the C-H stretching of sp3, which appeared at 2948 cm-1, C=O of the amides at 1615.8 cm^{-1}, and C-N stretching peaks of the amine/amide family, which appeared at 1400 cm^{-1}. These peaks can be attributed to the proteins and the alkaloids present in the stem bark. After the synthesis, some characteristic peaks observed include: 3754.0 and 3136.2 cm^{-1}, which are peaks within the region of –OH and the N-H's stretching vibrations. Mohan *et al*. have attributed the reducing ability of silver by acacia gum extract to the hydroxyl group in the polymeric chain via an oxidation mechanism [34], which is consistent with our observed peak for the –OH group. Absorption at 2078.2 cm^{-1} corresponding to the - Diazo (RCH=N-N, stretching) peak was shifted from 2078.2 cm^{-1} to 2176.6 cm^{-1}.

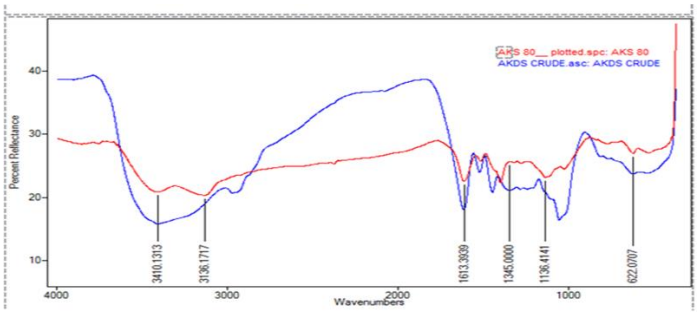

Figure 3. FTIR spectra of AKDS hydrosol and AKDS-AgNPs.

This could be attributed to the effect of resonance or conjugation of the diazo functional group. A Shift was also observed for the C-N bond (1284.6 to 1279.9 cm^{-1}), C-O-C bond (1213.8 to 1136.4cm^{-1}), and the N-O symmetric stretch (1345.9 to 1341.6 cm^{-1}). Other peaks include the O-H bend (950-910), 910-665 N-H wag, and the 900-675 C-H ("oops") bending vibrations [35]. These functional groups' synergistic effects could have reduced the metallic salt and subsequent capping of the nanoparticles. The spectral changes indicate the bioreduction and capping ability of Acacia karroo in synthesizing silver nanoparticles.

3.3. Morphological characterization.

3.3.1. SEM and EDS study.

The morphology of the synthesized nanoparticles was further characterized by a scanning electron microscope (SEM). Figures 4a and b show the micrograph of the crude

sample and the synthesized nanoparticles. The micrograph showed that the silver nanoparticles are spherical and polydispersed with large agglomeration. A similar observation was reported using the extract of *Ocimum sanctum* [36] and *Ipomoea indica* flowers [37].

Table 2. Changes in absorption bands in AKDS and as-synthesized AKDS-AgNPs.

AKDS (cm^{-1})	AKDS-AgNPs (cm^{-1})	Functional groups inference	Ref.
3409.8	3410.1	-OH or NH of tertiary amines	[38]
Absent	3136.2	-OH or NH vibrations of 1°, 2° amines, amides or alcohol	[39]
2948.0	2927.9	C-H asymmetric stretch of CH_3	[40]
2078.2	2173.7	RCH=N=N stretching of the diazo compounds	[41]
1883.0	Disappear	5-membered pyran resulting from the pyranose group/ Ag-O bond	[38,42]
1615.8	1613.4	C=O of the amides from the proteins	[42]
1522.0	1515.9	C=C-C aromatic ring stretch common to chromone moieties of the flavonoids	[42]
1447.9	1400.0	C-N bonds of the amino groups/ symmetric vibrations of the carboxylate group (-COO-)	[43]
1345.9	1341.6	N-O Aromatic nitro groups	[38]
1284.6	1279.9	C-N bonds of aliphatic amines	[39]
1213.8	1136.4	C-O stretch of phenol	[38]
1055.8	Disappear	-C-O stretch of alcohols	[43]
1034.9	1028.3	-OCH_3 of the ether linkage in the chromones	[44]
900-540	Below 800	C-H bending of the Vinyl group, C-halogen bonds stretch, C-H "oops" of aromatic, N-H wag of 1° and 2° amines	[38]

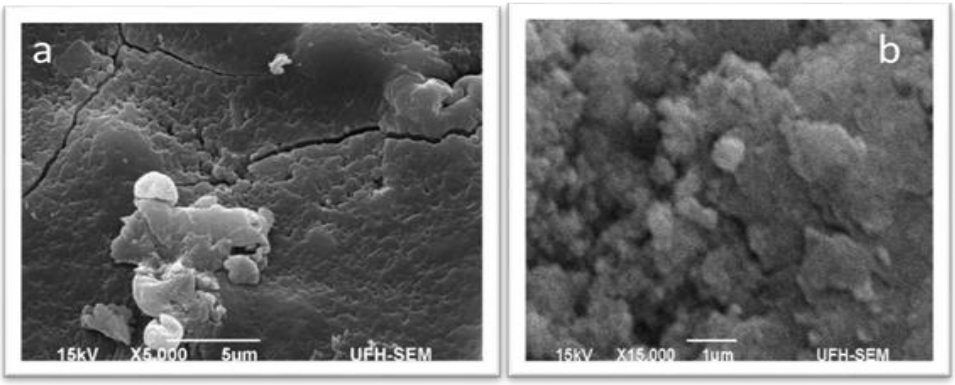

Figure 4. SEM analysis of **(a)** *AKDS hydrosol*; **(b)** *AKDS*- AgNPs.

Figure 5a and b show the dispersive energy spectrum of the AKDS-AgNPs, which confirms the presence of silver. The relative weights of the respective metals are shown as well. Metallic nanocrystals mostly display a distinctive optical absorption peak at 3 keV due to SPR. They can thus be confirmed for the silver formation in the nanoparticles.

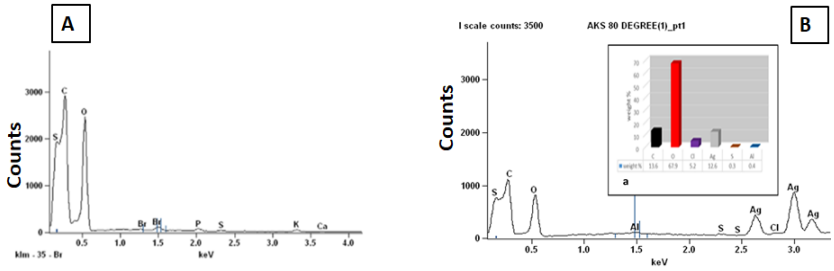

Figure 5. EDS spectra of AKDS **(A)** pure sample; **(b)** as-synthesized AKDS-AgNPs at 60°C.

3.3.2. XRD and TEM studies.

The crystalline nature of the dried powder of the as-synthesized Ag-NPs was confirmed by X-ray diffraction analysis. The XRD pattern shows a number of Bragg reflections that can be indexed on the face-centered cubic (fcc) of silver. The peaks at the 2θ degree values of

38.37°, 44.35°, 64.60°, 77.06°, and 81.39° correspond to (111), (200), (220), (311), and (222), respectively, when compared to the standard silver nanocrystals (JCPDS card No: 89- 3722).

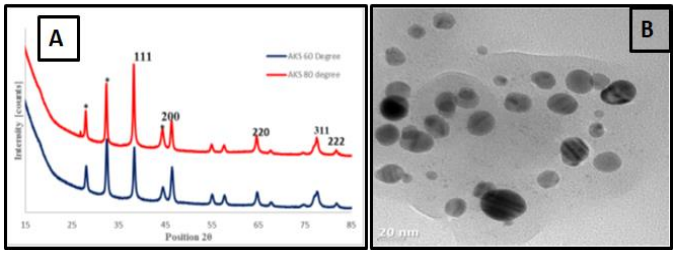

Figure 6. (A) A typical XRD pattern of AKDS-AgNPs synthesized at 60°C and 80°C; **(B)** HRTEM image of AKDS-AgNPs.

The unassigned peaks at 28.03°, 32.50°, and 46.47° may be ascribed to the bio-crystalline components or the amorphous bio-organic phase on the silver nanoparticles' surface inversely [36]. The lack of any peaks resembling metals apart from pure silver in the spectra confirmed the purity of the synthesized Ag-NPs. Also, peak broadening indicated the monocrystalline nature and smaller particle sizes. The calculated average crystallite size shows that increasing the reaction temperature from 60°C to 80°C led to an increase in size from 17.82 nm to 20.34 nm. This is attributed to the fact that, as smaller particles form at this temperature, they readily agglomerate into larger nanoparticles via Ostwald ripening.

Figure 6 (B) shows the TEM images of the silver nanoparticles synthesized from the Acacia karroo dry stem. The nanoparticles are spherical, polydisperse, and some irregular shapes at 100 nm; however, images at 20 nm show well-dispersed, spherical nanoparticles. The black spots on the nanoparticles' surface could be attributed to the metabolites' capping effect on the plant material. Mohan *et al*. reported earlier that silver nanoparticles are captured within the acacia core-shell structure. A phenomenon attributed entirely to the electrostatic and steric effects of the carboxylate groups of the polymeric chains in the acacia species [34].

3.4. Animal study.

3.4.1. Toxicity activity.

The AKDS and AKDS-AgNPs acute toxicity, evaluated at 50, 100, and 200 mg/kg body weight, had no adverse effects on the tested mice's behavioral responses after 14 days of observation. No mortality, size, or weight changes were noted. As a result, the maximum dosage of 200 mg/kg was selected. In this study, it was considered safe. The absence of these signals between animal groups suggests that the extract is not toxic under these conditions. The report here agrees with Adedapo *et al*. on the biosafety of *A. karroo* [45]. Extract of *A. mearnsii* tested against brine shrimp lethality displayed an LC_{50} in the range of 31.25-112.36 µg/mL, indicating that the extract was non-toxic [46]. The loss of body weight is a sensitive marker of toxicity upon exposure to toxic substances. *A. nilotica* extracts administered at different concentrations displayed no mortality, no weight changes, nor physiological changes in mice [47].

3.4.2. Analgesics and the effect.

Silver has been commonly used for wound healing and dressing since ancient times. Silver nanoparticles have been shown to promote better healing by decreasing inflammation through cytokine modulation [23]. The unique actions of Interleukin-10 (IL-10) include the

secretion of pro-inflammatory cytokines and the inhibition of leukocyte migration to the inflammation site [48]. The mechanisms of wound healing and inflammation are closely related. It involves the formation of edema, followed by the mediation of inflammation mediators, such as cytokines, prostaglandins, NO, and histamines. The oral administration of aspirin, saline solution, AKDS hydrosol, and AKDS-AgNPs at a 200 mg/kg dose post administration of formalin into the hind paw of Wistar rats. Both extracts displayed a relatively moderate inhibition against the formalin at the neurogenic phase (0-5 mins). The early phase normally peaks at 0-5 min (neurogenic phase), during which the drug interacts with the opioid system, leading to the release of substance P via a central mechanism of inflammation, followed by a period of remission. Table 3 shows the rate of inhibition of the extracts at both phases. AKDS-AgNPs inhibited the cytokine proliferation at the neurogenic phase (51%), more than the AKDS hydrosol (38%), with a level of significance of $p<0.01$. The 2nd phase (anti-inflammatory) is characterized by the release of several inflammatory mediators inhibited by nonsteroidal anti-inflammatory drugs (NSAIDs) [49]. Thus, the mechanism of inhibition is compared to that of the NSAIDs. In this study, the AKDS-AgNPs displayed a lower than 39% when compared to the AKDS hydrosol (85%). The analgesic properties of the AK-AgNPs decrease during the inflammatory stage compared with the neurogenic phase. The rapid activity of the synthesized nanoparticles indicates that AKDS-AgNPs exhibit high absorption at the early stage of analysis, suggesting that they can be used as an opioid-regulatory drug.

Silver nanoparticles have been reported to adhere to cells by interaction with lipids. Initially, proteins and other cell membrane components followed the energy-dependent uptake process [50,51]. Other potential factors contributing to low inhibition during the inflammatory phase could include the dose, solubility, and inhibition rate.

Table 3. Antinociceptive effects of AKDS-Ag-NPs on formalin-induced pain.

		Neurogenic phase (0-5 mins)		Inflammatory phase (10-30 min)	
Treatment	**Dose (mg/kg)**	**No. of Licks**	**Inhibition (%)**	**No. of Licks**	**Inhibition (%)**
Control	Normal saline	42.3 ± 1.5		30.5 ± 1.7	
Standard (Aspirin)	100	7 ± 1.3 **	83	6.8 ± 1.4 **	78
AKDS crude	200	26 ± 2.1**	39	4.7 ± 1.3 **	85
AKDS-AgNPs	200	20.8 ± 0.8**	51	20± 2.9 **	39

Values expressed as mean ± SEM. (n=5), **p<0.01.

Conclusively, the synthesized Ag-NPs inhibited the analgesic and inflammation phases. However, the effect was more evident in the neurogenic (analgesic) phase. Also, nanoparticles synthesized from the stem bark of *Acacia mearnsii* inhibited pro-inflammatory mediators at a higher rate (71%) than opioids (51%) at the stage [32].

4. Conclusions

We have demonstrated the reductive and stabilizing ability of the hydrosol extract of *Acacia karoo* on silver nitrate to yield a nanoparticle having a mean diameter of 10-20 nm with optimum synthesis at a temperature of 80°C. The synthesized AgNPs significantly reduced pain and inflammation mediators at 51% and 39% for the neurogenic and inflammatory phases, respectively. This synthetic pathway is simple, economical, and void of hazardous chemicals. The bio-reductive and capping ability of the *Acacia karroo* hydrosols is attributed to the presence of biomolecules, of which tannins, flavonoids, and terpenoids are predominant. More robust research is ongoing to elucidate the mechanism underlying the pain-relieving effect

using several cytokines and to further understand the synthesized AKDS-AgNPs for drug delivery, cytotoxicity, and anticancer properties.

Author Contributions

Conceptualization, O.A.and FA.; methodology, FM; FA. software, Z.O.; A.A.; O.O.; validation, Z.O.; O.O.; O.A. formal analysis, F.M.; A.A.; Z.O.;investigation, O.A.; O.O; resources, O.A.; F.M.; data curation, A.A.; F.A. writing—original draft preparation, O.A .and O.O; writing—review and editing, F.M; A.A; O.O.; supervision, Z.O.; F.A; A.A.; All authors have read, reviewed, and agreed that the manuscript be published in this version.

Institutional Review Board Statement

The animal study protocol reported in this manuscript was approved by the Research Ethical Clearance Committee (RECC) of Lagos State University (Approval no: 013/2019/LASU/BCH).

Informed Consent Statement

Not applicable.

Data Availability Statement

Data supporting the findings of this study are available upon reasonable request from the corresponding author.

Funding

This research received no external funding.

Acknowledgments

The authors acknowledged the support of Mr. Akinpelu A. of the Chemistry Department, Lagos State University, for his assistance with the analysis of the samples.

Conflicts of Interest

The authors declare no conflict of interest.

References

1. Bora, M. Recent Bio-Medical Applications of Iron Oxide Magnetic Nanoparticles. *J. ISAS* **2023**, *1*, 56–72, https://doi.org/10.59143/isas.jisas.1.4.COWE4565.
2. Khorasani, A.; Shahbazi-Gahrouei, D.; Safari, A. Recent Metal Nanotheranostics for Cancer Diagnosis and Therapy: A Review. *Diagnostics* **2023**, *13*, 833, https://doi.org/10.3390/diagnostics13050833.
3. Sowmya, N.; Mohanty, D.; Nirosha, B.; Kumar, N.U.; Patra, P.K. A Systematic Review Of Metallic Nanoparticles: Synthesis, Biological Activities & Applications. *J. Pharm. Negat. Results* **2023**, *14*, 2525–2533, https://doi.org/10.47750/pnr.2023.14.S02.297.
4. Singh, A.; Banerjee, S.L.; Gantait, A.; Kumari, K.; Kundu, P.P. Metal-Based Nanoparticles: Synthesis and Biomedical Applications. In Nanoparticles Reinforced Metal Nanocomposites: Mechanical Performance and Durability, Tiwari, S.K., Kumar, V., Thomas, S., Eds.; Springer Nature Singapore: Singapore, **2023**; pp. 365-408, https://doi.org/10.1007/978-981-19-9729-7_13.

5. Villalobos Gutiérrez, P.; Muñoz Carrillo, J.; Sandoval Salazar, C.; Viveros Paredes, J.; Gutiérrez Coronado, O. Functionalized Metal Nanoparticles in Cancer Therapy. *Pharmaceutics* **2023**, *15*, 1932, https://doi.org/10.3390/pharmaceutics15071932.
6. Saadh, M.J. Silver Nanoparticles Inhibit Goatpox Virus Replication. *Arch. Virol.* **2023**, *168*, 32, https://doi.org/10.1007/s00705-022-05667-5.
7. Gupta, D.; Boora, A.; Thakur, A.; Gupta, T.K. Green and Sustainable Synthesis of Nanomaterials: Recent Advancements and Limitations. *Environ. Res.* **2023**, *231*, 116316, https://doi.org/10.1016/j.envres.2023.116316.
8. Sukul, P.K.; Kar, C. Green Conversion Methods to Prepare Nanoparticle. In Bioinspired and Green Synthesis of Nanostructures; Scrivener Publishing LLC: **2023**; pp. 115-139, https://doi.org/10.1002/9781394174928.ch5.
9. Singh, A.K.; Talat, M.; Singh, D.P.; Srivastava, O.N. Biosynthesis of Gold and Silver Nanoparticles by Natural Precursor Clove and Their Functionalization with Amine Group. *J. Nanoparticle Res.* **2010**, *12*, 1667–1675, https://doi.org/10.1007/s11051-009-9835-3.
10. Ahmad, N.; Sharma, S.; Alam, Md.K.; Singh, V.N.; Shamsi, S.F.; Mehta, B.R.; Fatma, A. Rapid Synthesis of Silver Nanoparticles Using Dried Medicinal Plant of Basil. *olloids Surf. B: Biointerfaces* **2010**, *81*, 81–86, https://doi.org/10.1016/j.colsurfb.2010.06.029.
11. Makarov, V.V.; Love, A.J.; Sinitsyna, O.V.; Makarova, S.S.; Yaminsky, I.V.; Taliansky, M.E.; Kalinina, N.O. "Green" nanotechnologies: synthesis of metal nanoparticles using plants. *Acta Naturae* **2014**, *6*, 35-44.
12. Velmurugan, P.; Anbalagan, K.; Manosathyadevan, M.; Lee, K.J.; Cho, M.; Lee, S.M.; Park, J.H.; Oh, S.G.; Bang, K.S.; Oh, B.T. Green Synthesis of Silver and Gold Nanoparticles Using Zingiber Officinale Root Extract and Antibacterial Activity of Silver Nanoparticles against Food Pathogens. *Bioprocess Biosyst. Eng.* **2014**, *37*, 1935–1943, https://doi.org/10.1007/s00449-014-1169-6.
13. Kora, A.J.; Beedu, S.R.; Jayaraman, A. Size-controlled green synthesis of silver nanoparticles mediated by gum ghatti (*Anogeissus latifolia*) and its biological activity. *Org. Med. Chem. Lett.* **2012**, *2*, 17, https://doi.org/10.1186/2191-2858-2-17.
14. Maione, F. Targeting Inflammation and Inflammatory-Related Diseases with Natural Bioactives; MDPI: Basel, Switzerland, **2023**; https://doi.org/10.3390/books978-3-0365-7296-3.
15. Serebrennikova, S.N. INFLAMMATION AS A FUNDAMENTAL PATHOLOGICAL PROCESS: LECTURE 1 (ALTERATION, VASCULAR REACTIONS). *Baikal Med. J.* **2023**, *2*, 53–64, https://doi.org/10.57256/2949-0715-2023-2-53-64.
16. Kumari, P.; Kumar, H. Dimensions of Inflammation in Host Defense and Diseases. *Int. Rev. Immunol.* **2022**, *41*, 1–3, https://doi.org/10.1080/08830185.2022.2014174.
17. Arfeen, M.; Srivastava, A.; Srivastava, N.; Khan, R.A.; Almahmoud, S.A.; Mohammed, H.A. Design, Classification, and Adverse Effects of NSAIDs: A Review on Recent Advancements. *Bioorg. Med. Chem.* **2024**, *112*, 117899, https://doi.org/10.1016/J.BMC.2024.117899.
18. Stone, S.; Malanga, G.A.; Capella, T. Corticosteroids: Review of the History, the Effectiveness, and Adverse Effects in the Treatment of Joint Pain. *Pain Physician* **2021**, *24*, S233–S246.
19. Andleeb, S.; Iqbal, epub; Gulzar, N.; Raza, A.; Ahmad, A. Synthesis, Characterization, Acute Dermal Toxicity, Anti-Inflammatory, and Wound Healing Potential of Biogenic Silver Nanoparticles in Balb C Mice. *Curr. Pharm. Biotechnol.* **2023**, *25*, 1452–1465, https://doi.org/10.2174/1389201024666230727122201.
20. Takem, L.P.; Lawal, B.A.S.; Udia, P.M. Analgesic and Acute Anti-inflammatory Activities of Aqueous Root Extract of Salacia lehmbachii. *J. Pharma. Res. Int.* **2014**, *4*, 2172–2181, https://doi.org/10.9734/BJPR/2014/9250.
21. Nadworny, P.L.; Wang, J.; Tredget, E.E.; Burrell, R.E. Anti-Inflammatory Activity of Nanocrystalline Silver-Derived Solutions in Porcine Contact Dermatitis. *J. Inflamm.* **2010**, *7*, 13, https://doi.org/10.1186/1476-9255-7-13.
22. Luceri, A.; Francese, R.; Lembo, D.; Ferraris, M.; Balagna, C. Silver Nanoparticles: Review of Antiviral Properties, Mechanism of Action and Applications. *Microorganisms* **2023**, *11*, 629, https://doi.org/10.3390/MICROORGANISMS11030629.
23. Tian, J.; Wong, K.K.Y.; Ho, C.M.; Lok, C.N.; Yu, W.Y.; Che, C.M.; Chiu, J.F.; Tam, P.K.H. Topical Delivery of Silver Nanoparticles Promotes Wound Healing. *ChemMedChem* **2007**, *2*, 129–136, https://doi.org/10.1002/CMDC.200600171.

24. Van Wyk, B.-E;. van Oudtshoorn, B.; Gericke, N. Medicinal Plants of South Africa; Briza Publications: Pretoria, South Africa, **1997**.
25. Dold, A.P.; Cocks, M.L. Traditional veterinary medicine in the Alice district of the Eastern Cape Province, South Africa: Research in action. *S. Afr. J. Sci.* **2001**, *97*, 375-379, https://hdl.handle.net/10520/EJC97371.
26. Mogole, L.; Omwoyo, W.; Mtunzi, F. Phytochemical Screening, Anti-Oxidant Activity and α-Amylase Inhibition Study Using Different Extracts of Loquat (Eriobotrya Japonica) Leaves. *Heliyon* **2020**, *6*, e04736, https://doi.org/10.1016/j.heliyon.2020.e04736.
27. Prabhu, V.V.; Nalini, G.; Chidambaranathan, N.; Kisan, S.S. Evaluation of anti-inflammatory and analgesic activity of Tridax procumbens Linn against formalin, acetic acid and CFA induced pain models. *Int. J. Pharm. Pharm. Sci.* **2011**, *3*, 126-130.
28. Nyila, M.; Leonard, C.; Hussein, A.; N., L. Activity of South African Medicinal Plants against Listeria Monocytogenes Biofilms, and Isolation of Active Compounds from. Acacia Karroo. *S. Afr. J. Bot.* **2012**, *78*, 220-227, https://doi.org/10.1016/j.sajb.2011.09.001.
29. Murugan, K.; Senthilkumar, B.; Senbagam, D.; Al-sohaibani, S. Biosynthesis of Silver Nanoparticles Using Acacia Leucophloea Extract and Their Antibacterial Activity. *Int. J. Nanomed.* **2014**, *9*, 2431–2438, https://doi.org/10.2147/IJN.S61779.
30. Baranitharan, M.; Alarifi, S.; Alkahtani, S.; Ali, D.; Elumalai, K.; Pandiyan, J.; Krishnappa, K.; Rajeswary, M.; Govindarajan, M. Phytochemical Analysis and Fabrication of Silver Nanoparticles Using Acacia Catechu: An Efficacious and Ecofriendly Control Tool against Selected Polyphagous Insect Pests. *Saudi J. Biol. Sci.* **2021**, *28*, 148–156, https://doi.org/10.1016/j.sjbs.2020.09.024.
31. Rajesh, K.M.; Neelu, C. Green Synthesis of Silver Nanoparticles Using Acacia Concinna Plant extract and Their Antibacterial Activity. *Res. J. Recent Sci.* **2018**, *7*, 1-6.
32. Avoseh, O.N.; Oyedeji, O.O.; Aremu, O.; Nkeh-Chungag, B.N.; Songca, S.P.; Oyedeji, A.O.; Mohan, S.; Oluwafemi, O.S. Biosynthesis of Silver Nanoparticles from Acacia Mearnsii De Wild Stem Bark and Its Antinociceptive Properties. *Green Chem. Lett. Rev.* **2017**, *10*, 59-68, https://doi.org/10.1080/17518253.2017.1287310.
33. Liu, H.; Zhang, H.; Wang, J.; Wei, J. Effect of Temperature on the Size of Biosynthesized Silver Nanoparticle: Deep Insight into Microscopic Kinetics Analysis. *Arab. J. Chem.* **2020**, *13*, 1011–1019, https://doi.org/10.1016/j.arabjc.2017.09.004.
34. Mohan, Y.M.; Raju, K.M.; Sambasivudu, K.; Singh, S.; Sreedhar, B. Preparation of Acacia-Stabilized Silver Nanoparticles : A Green Approach. *J. Appl. Polym. Sci.* **2007**, *106*, 3375–3381, https://doi.org/10.1002/app.26979.
35. Thilagam, M.; Tamilselvi, a; Chandrasekeran, B.; Rose, C. Phytosynthesis of Silver Nanoparticles Using Medicinal and Dye Yielding Plant of Bixa Orellana L. Leaf Extract. *J. Pharm. Sci. Innov.* **2013**, *2*, 9–13, https://doi.org/10.7897/2277-4572.02441.
36. Rout, Y. Green Synthesis of Silver Nanoparticles Using Ocimum Sanctum (Tulashi) and Study of Their Antibacterial and Antifungal Activities. *J. Microbiol. Antimicrob.* **2012**, *4*, 103–109, https://doi.org/10.5897/JMA11.060.
37. Pavani, K. V; Gayathramma, K.; Banerjee, A.; Suresh, S. Phyto-Synthesis of Silver Nanoparticles Using Extracts of Ipomoea Indica Flowers. *Am. J. Nanomater.* **2013**, *1*, 5–8.
38. Coates, J. Interpretation of Infrared Spectra, A Practical Approach. In Encyclopaedia of Analytical Chemistry; Meyers, R.A., Ed.; John Wiley & Sons Ltd, Chichester, **2000**; pp. 10815–10837.
39. Gnanajobitha, G.; Paulkumar, K.; Vanaja, M.; Rajeshkumar, S.; Malarkodi, C.; Annadurai, G.; Kannan, C. Fruit-Mediated Synthesis of Silver Nanoparticles Using Vitis Vinifera and Evaluation of Their Antimicrobial Efficacy. *J. Nanostruct. Chem.* **2013**, *3*, 67, https://doi.org/10.1186/2193-8865-3-67.
40. Ajitha, B.; Ashok Kumar Reddy, Y.; Sreedhara Reddy, P. Biosynthesis of Silver Nanoparticles Using Plectranthus Amboinicus Leaf Extract and Its Antimicrobial Activity. *Spectrochim. Acta A Mol. Biomol. Spectrosc.* **2014**, *128*, 257–262, https://doi.org/10.1016/j.saa.2014.02.105.
41. Subramani, V.; Jeyakumar, J.J.; Kamaraj, M.; Ramachandran, B. Plant Extracts Derived Silver Nanoparticles. *Int. J. Pharma. Res. Rev.* **2014**, *3*, 16–19.
42. Shameli, K.; Bin Ahmad, M.; Jaffar Al-Mulla, E.A.; Ibrahim, N.A.; Shabanzadeh, P.; Rustaiyan, A.; Abdollahi, Y.; Bagheri, S.; Abdolmohammadi, S.; Usman, M.S. Green biosynthesis of silver nanoparticles using Callicarpa maingayi stem bark extraction. *Molecules* **2012**, *17*, 8506-8517, https://doi.org/10.3390/molecules17078506.

43. Panda, K.K.; Achary, V.M.M.; Krishnaveni, R.; Padhi, B.K.; Sarangi, S.N.; Sahu, S.N.; Panda, B.B. In Vitro Biosynthesis and Genotoxicity Bioassay of Silver Nanoparticles Using Plants. *Toxicol. In Vitro* **2011**, *25*, 1097–1105, https://doi.org/10.1016/j.tiv.2011.03.008.
44. Huang, J.; Li, Q.; Sun, D.; Lu, Y.; Su, Y.; Yang, X.; Wang, H.; Wang, Y.; Shao, W.; He, N. Biosynthesis of silver and gold nanoparticles by novel sundried Cinnamomum camphoraleaf. *Nanotechnology* **2007**, *18*, 105104, https://doi.org/10.1088/0957-4484/18/10/105104.
45. Adedapo, A.A.; Sofidiya, M.O.; Masika, P.J.; Afolayan, A.J. Safety Evaluations of the Aqueous Extract of Acacia Karroo Stem Bark in Rats and Mice. *Rec. Nat. Prod.* **2008**, *2*, 128–134.
46. Olajuyigbe, O.O.; Afolayan, A.J. Pharmacological Assessment of the Medicinal Potential of Acacia Mearnsii de Wild: Antimicrobial and Toxicity Activities. *Int. J. Mol. Sci.* **2012**, *13*, 4255–4267, https://doi.org/10.3390/ijms13044255.
47. Mohan, S.; Thiagarajan, K.; Chandrasekaran, R.; Arul, J. In Vitro Protection of Biological Macromolecules against Oxidative Stress and in Vivo Toxicity Evaluation of Acacia Nilotica (L .) and Ethyl Gallate in Rats. *BMC Complement Altern. Med.* **2014**, *14*, 257, https://doi.org/10.1186/1472-6882-14-257.
48. Sun, R.W.-Y.; Chen, R.; Chung, N.P.-Y.; Ho, C.-M.; Lin, C.-L.S.; Che, C.-M. Silver nanoparticles fabricated in Hepes buffer exhibit cytoprotective activities toward HIV-1 infected cells. *Chem. Commun.* **2005**, 5059-5061, https://doi.org/10.1039/B510984A.
49. Nkeh-chungag, B.N.; Ndebia, E.J.; Mbafor, J.T.; Dotwana, L.A.; Oyedeji, O.O.; Iputo, J.E. The effect of *Cordia platythyrsa* on various experimental models of pain and carrageenan induced inflammation. *Afr. Biotechnol.* **2014**, *13*, 343–348, https://doi.org/10.5897/AJB2013.13018.
50. Chithrani, B.D.; Ghazani, A.A.; Chan, W.C.W. Determining the Size and Shape Dependence of Gold Nanoparticle Uptake into Mammalian Cells. *Nano Lett.* **2006**, *6*, 662–668, https://doi.org/10.1021/nl052396o.
51. Lesniak, A.; Salvati, A.; Santos-Martinez, M.J.; Radomski, M.W.; Dawson, K.A.; Åberg, C. Nanoparticle Adhesion to the Cell Membrane and Its Effect on Nanoparticle Uptake Efficiency. *J. Am. Chem. Soc.* **2013**, *135*, 1438–1444, https://doi.org/10.1021/ja309812z.

Publisher's Note & Disclaimer